CDF/ANAL/MUON/CDFR/726
September 14, 1988

Decay-in-Flight Acceptance of the Central Muon Chambers

David A. Smith and Thomas K. Westhusing
University of Illinois

Abstract

The decay of pions and kaons into muons is simulated using CDFSIM, and then the full, standard event reconstruction is applied in order to calculate the acceptance of the central muon chambers for secondary muons.

1 Why Use the Monte Carlo?

The probability for a pion or a kaon to decay to a muon, via the processes

$$\pi \rightarrow \mu\nu, \qquad K \rightarrow \mu\nu$$

is simply

$$\mathcal{P}(p_t) = 1 - e^{-Mr/c\tau p_t} \approx \frac{Mr}{c\tau p_t} \tag{1}$$

where $c\tau$ is the decay length, r is the distance from the beam axis traveled by the meson, M is the meson mass, and p_t is the transverse momentum of the meson [1]. Values are listed in table 1. (The approximation is valid for $r = R_{cmu}$ and the momentum acceptance of the central muon chambers, and improves with increasing p_t.)

Furthermore, the energy distribution of the decay muons is flat over the range of kinematically allowed energies E_μ, which is

$$f_i E_{meson} \leq E_\mu \leq E_{meson},$$
$$\text{where } f_\pi = 0.57 \text{ for pions and } f_K = 0.05 \text{ for kaons,}$$

and where E_{meson} is the energy of the primary pion or kaon. Hence, given the geometry of the central muon coverage and the branching ratios for K or $\pi \rightarrow \mu\nu$, one should be able to calculate the probability that muons above some momentum threshold reach the muon chambers, without resorting to complicated monte carlo's.

But the above gives only a rough estimate of the decay muon acceptance. Three principal effects muddy the picture (see figure 1):

[1] Throughout this note, 'transverse momentum' means transverse relative to the beam axis.

	M (MeV)	$c\tau$ (cm)	$mR_{cmu}/c\tau$ (MeV)	$B.R.$
$\pi^{\pm}$	139.6	780.4	62.1	100 %
$K^{\pm}$	493.7	370.9	461.9	63.5 %

Table 1: Some properites of kaons and pions. $R_{cmu} = 347$ cm is the radius of the central muon chambers. $B.R.$ is the branching ratio to $\mu\nu$.

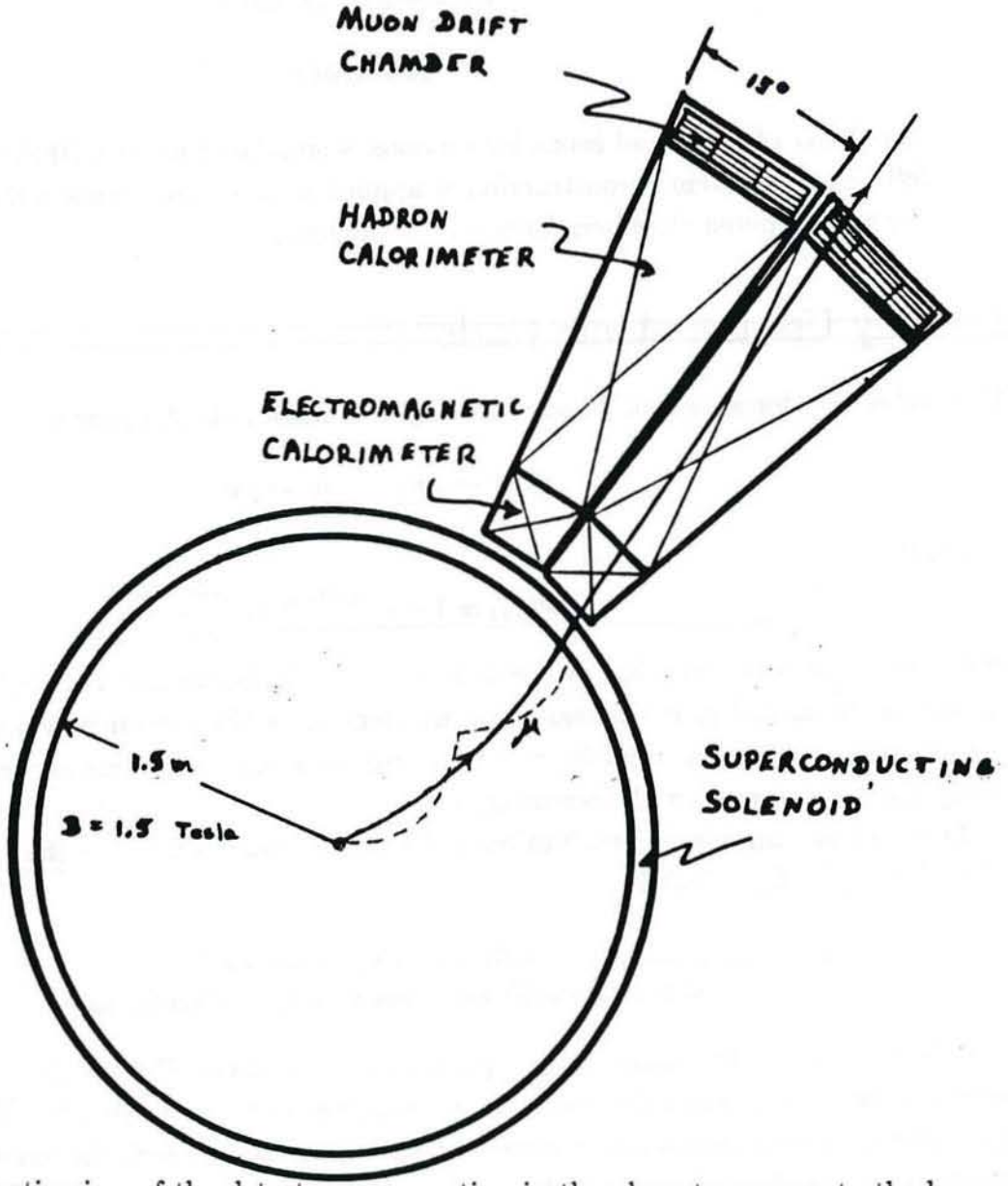

Figure 1: Schematic view of the detector cross section in the plane transverse to the beam axis, showing the central tracking chamber, calorimeter wedges, and muon chambers. The dashed curve represents a primary meson track and a secondary muon track with a 'kink' at the decay vertex. The solid line is a possible single track fit to the combined meson and muon tracks. Track curvatures in the axial magnetic field are exaggerated for clarity [1].

1. **Low Secondary Momentum** The decay muons have lower momenta than the parent mesons, so some of the secondary muons will fail the muon identification cuts because
   - the track may fail the p_t cut;
   - increased multiple scattering for the soft secondary could cause it to fail the CTC/CMU track matching cuts;
   - $\frac{dE}{dx}$ losses in the calorimeter cause some muons to range out before reaching the muon chambers. Range-out energy of a muon traversing an entire wedge is 1.4 GeV/$\sin\theta$.
2. **Kinks** The decaying meson gives the muon a 'kick' in the direction transverse to the parent momentum, which can produce a 'kink' in the track, with different consequences:
   - The central tracking pattern recognition code may not recognize two distinct tracks, and will instead fit the parent and secondary tracks to a single track with some 'compromise' momentum value. Figure 3 shows momentum distributions for tracks reconstructed from mesons that were forced to decay in the simulation. Note that some tracks have higher momenta than their parents!
   - The transverse kick can send the muon astray, so that it fails the CTC/CMU track matching cuts. Coupled with the increased multiple scattering of the soft secondaries, this is a non-negligible effect.
   - The reconstructed track will have an impact parameter or residuals values that cause the track to fail quality cuts.
3. $\frac{dE}{dx}$ **losses** slow the meson down and thereby increase its decay probability. This is a small correction to the total rate, but for low momentum mesons it decreases the magnitude of the expected charge asymmetry, discussed later in this note and in reference [3].

CDFSIM, the CDF detector simulation, includes these effects and allows for a more realistic calculation of the decay acceptance.

Earlier work by Skarha showed negligible stiffening of the minimum bias dN/dp_t distribution due to misreconstruction of kinked tracks [4]. Muon data, however, contains more decay contamination and the effect is larger.

2 The Method

The shape of the observed momentum distribution for decay muons,

$$(\frac{dN_\mu}{dp_t})_{obs}, \tag{2}$$

depends on the shape of the parent meson distribution, $\frac{dN}{dp_t}$, which will be different for different physics studies (i.e., min bias, jets, vector bosons, etc). Rather than choosing a specific parametrization for $\frac{dN}{dp_t}$, we have adopted a more general approach.

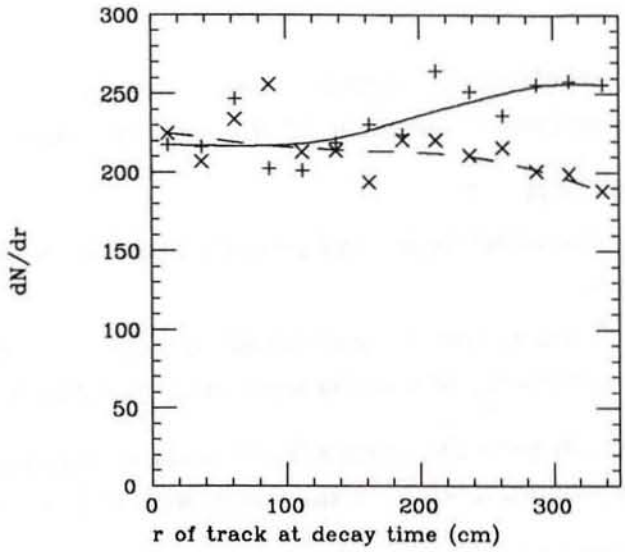

Figure 2: Distribution of radii at which a parent meson decays into a muon. The solid curve (+'s) includes the dE/dx losses that slow down the parent mesons, thereby increasing the decay probability in the calorimeter. The dashed curve (X's) is uncorrected. The two curves are the same until the beginning of the calorimeter ($r \simeq 150$ cm). The curves are only intended to guide the eye.

2.1 Event Generation

FAKEV generates 3000 mesons at each of 24 transverse momentum. The transverse momenta are

$$p_t^{meson} = (2, 3, 4, ..., 19, 20, 22, 24, ...30)\text{GeV/c}. \tag{3}$$

The meson distributions in azimuth angle ϕ and in pseudorapidity $|\eta| < 1.1$ are flat. The η interval is larger than the range covered by the central muon chambers, $|\eta| < 0.65$, to allow for secondary muons scattered to wide angles in the rz-plane of the detector.

FAKEV also selects the decay radius for the meson according to the distribution shown in figure 2 (solid curve). The decay radius r_{dk} is the distance traveled by the meson before the simulation forces the particle to decay,

$$0 < r_{dk} < R_{cmu}, \qquad R_{cmu} = 347\text{cm},$$

where R_{cmu} is the innnermost radius of the central muon chambers. As CDFSIM steps a particle through the layers of the detector, it compares the current radial position r of the particle with r_{dk}, and if $r \geq r_{dk}$ then the program forces the decay of the particle. However, if the meson has already showered then decay will not occur. In this way we correctly find the fraction of mesons that decay before reaching the muon chambers.

Figure 2 shows the distribution of decay radii for simulated 7 GeV/c kaons. The dashed curve is the distribution that comes from equation (1), for fixed p_t. The solid curve includes a correction for the dE/dx losses of the meson. As a meson traversing the calorimeter slows

CTC Track Cuts		
D_0	Δz_{vtx}	p_t
0.5 cm	5.0 cm	2.0 GeV/c

	CTC/CMU Match Cuts		
	dx	dz	$d\alpha$
loose	20. cm	20. cm	0.2 rad
tight	8. cm	15. cm	0.06 rad

Table 2: Values of the cuts made on the CTC tracks, and on the match between the CTC track and the CMU stub. The parameters are described in the text.

down due to multiple coulomb interactions, its decay probability per unit distance increases. The r-dependence of p_t in equation (1) is included in the calculation. The solid and dashed curves are the same until the beginning of the calorimeter ($r \simeq 150$ cm) and differ by about 20% at the muon chambers.

2.2 Track Reconstruction

After simulating the propagation of the mesons and their daughters through the detector, the results are analysed with the same programs used for events from $p\bar{p}$ collisions. That is, we reconstruct the 'stubs' in the muon chambers, reconstruct the CTC tracks using the vertex-constrained fit, extrapolate the CTC track through the calorimeter (including effects of the return magnetic field in the steel), and then match the closest track/stub pair at the muon chambers. Even these very simple events produce multiple CTC tracks and muon stubs: multiple tracks arise if the decay kink is so large that the reconstruction algorithm resolves two tracks, and multiple stubs can come from knock-on electrons produced in the chamber walls. The resulting track/stub matches are considered muon-candidates, and figure 3 shows the distributions of observed transverse momenta for each of the parent meson momenta.

Cuts are made on both the CTC track quality and on the CTC/CMU match. Table 2 lists the cut values. D_0 is the distance of closest approach of the track to the collision vertex in the $r\phi$-plane of the detector (impact parameter). In the rz-plane, $\Delta z_{vtx} = |z_{p\bar{p}} - z_{trk}|$ is the distance between the collision vertex and the z-coordinate of the track at $r = 0$. The transverse momentum p_t is the observed value as measured by the CTC track reconstruction code. The CTC/CMU matching parameters dx, dz are the differences, in centimeters, between the CMU stub and the extrapolated CTC track at the muon chambers, in the ϕ-direction and along the beam axis, respectively. $d\alpha$ is the slope difference in the $r\phi$-plane between the CMU stub and the CTC track.

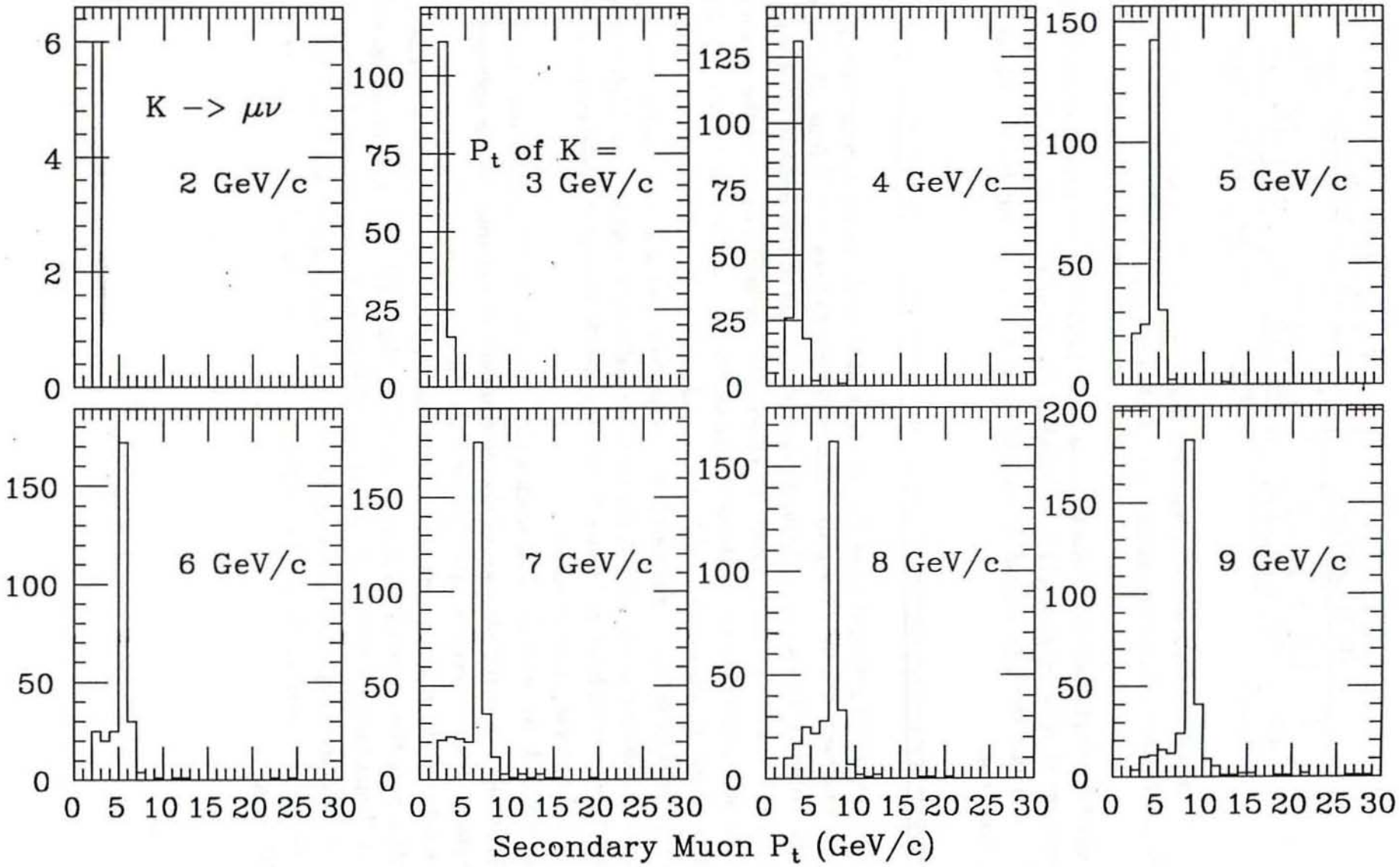

Figure 3: Transverse momentum distributions for muons coming from the decay of simulated kaons and passing the 'loose' cuts of table 2. Primary kaon p_t is shown in each plot. The central track reconstruction code yields distributions different from those predicted by kinematics.

Given the plots in figure 3, one can calculate the observed muon momentum distribution (equation 2) for an arbitrary parent distribution, using the recipe

$$N(p_t^\mu) = \frac{1}{3000} \sum_j d_j n_j(p_t^\mu) m(p_j^K) \tag{4}$$

where $N(p_t^\mu)$ is the observed number of muons with transverse momentum p_t^μ;
3000 is the number of generated parent mesons;
j is an index running over the meson momenta of equation (3);
p_j^K is the parent meson transverse momentum for the j^{th} plot in figure 3;
d_j is the probability for the meson to decay before the muon chambers;
$n_j(p_t^\mu)$ is the number of entries in the p_t^μ bin of the j^{th} plot in figure 3;
$m(p_j^K)$ is the number of parent mesons with momentum p_j^K.

Restated, the factor $d_j n_j(p_t^\mu)/3000$ is the probability of a parent meson of momentum p_j^K producing a muon with momentum p_t^μ.

For the dashed curve in figure 2, $d_j = (1 - e^{-MR_{cmu}/c\tau p_j^K})$, using the constants listed in table 1. But in the dE/dx corrected simulation, d_j is a constant calculated in the simulation, and is typically 10% larger than d_j for no dE/dx.

3 Sample Calculations

We illustrate equation (4) with two examples, namely, a flat momentum distribution for the parent mesons, and a distribution like the one for the charged tracks in the 1987 jet data.

3.1 Flat Input Spectrum

In this case, $m(p_j^K) = 1$ for all j in equation (4). Figure 4 shows $N(p_t^\mu)$ for kaons, for two different sets of track/stub matching cuts. The cuts are listed in table 2.

3.2 Jet $\frac{dN}{dp_t}$ Distribution

In this case, $m(p_j^K)$ in equation (4) comes from a rapidly falling distribution, typical of the charged tracks in 1987 jet data. Figure 5 shows the resulting secondary muon spectrum, for two extreme choices of the $\frac{K}{\pi}$ ratio [2]. The muons have passed the tight cuts of table 2. The total rate is fairly insensitive to the particle mix, which is simply a reflection of the fact that the acceptances for kaons and pions separately are comparable.

3.3 Do-It-Yourself

The interested reader will have a parent $\frac{dN}{dp_t}$ distribution of his own, for which he will want to calculate the observed secondary muon spectrum. A standalone Fortran program that reads the

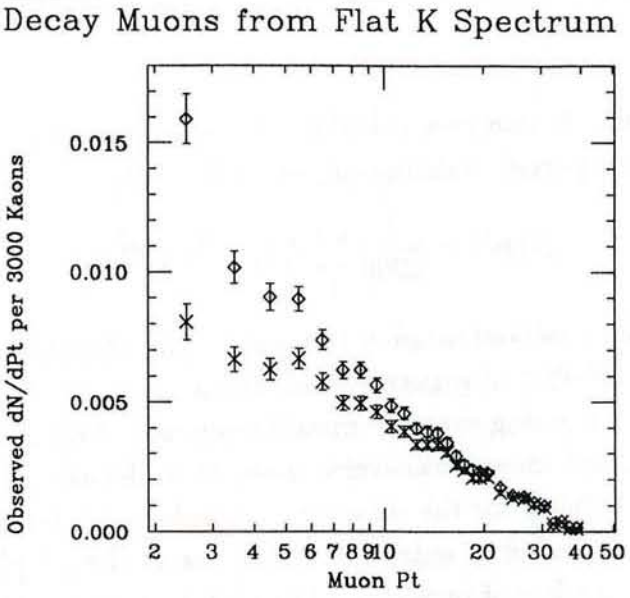

Figure 4: Acceptance for muons from kaon decay-in-flight assuming a flat distribution of parent momenta. In the top curve, loose cuts for the match between the CTC track and the CMU stub have been applied, while the lower curve had tight cuts. The cuts are defined in the text.

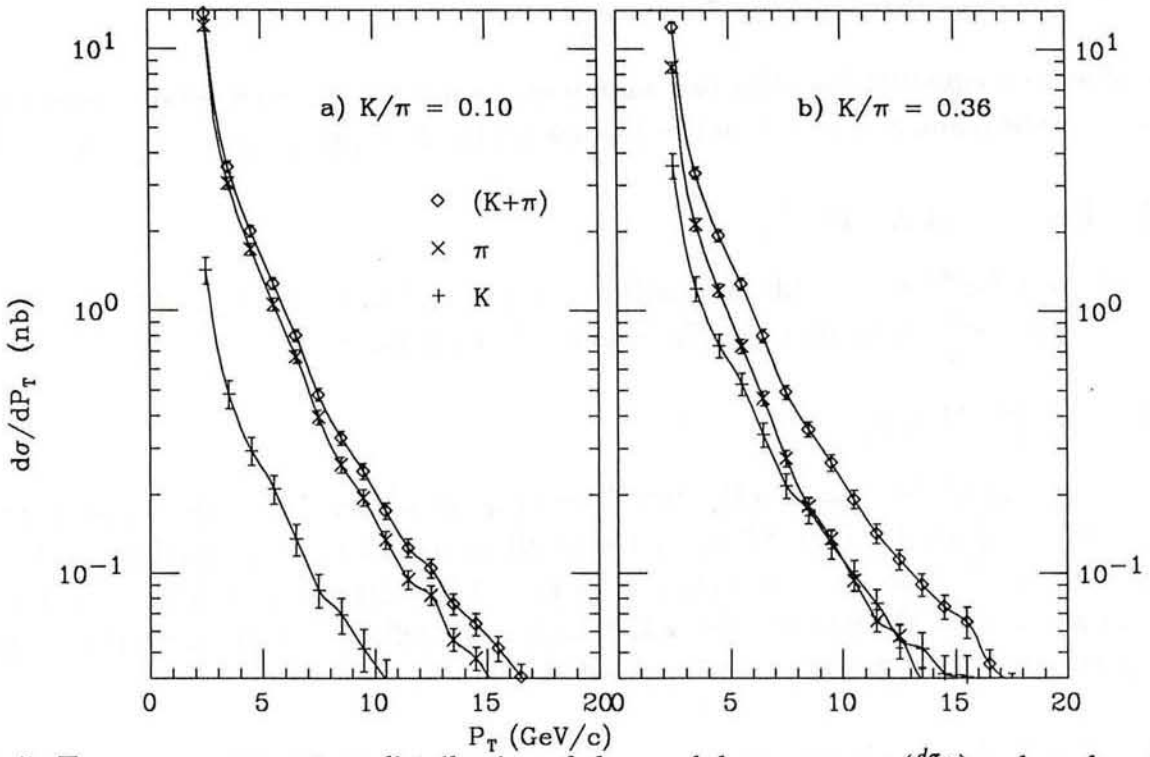

Figure 5: Transverse momentum distribution of observed decay muons, $(\frac{d\sigma_\mu}{dp_t})_{obs}$, based on a parent meson distribution similar to that of charged tracks in jet events. The contributions from pions and kaons are shown, together with the sum of the two, for two different particle mixtures.

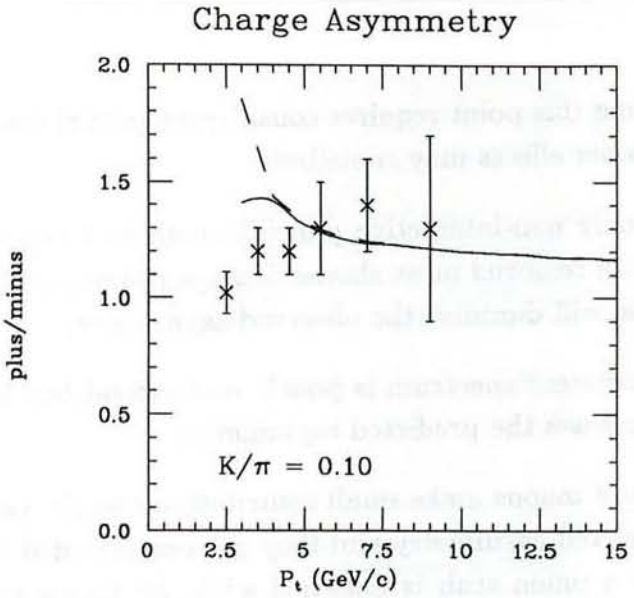

Figure 6: Charge asymmetry in the central muon chambers. The curves combine non-interactive punchthrough [3] with meson decay-in-flight. The solid curve includes the meson dE/dx losses in the calorimeter, while the dashed curve is uncorrected. The points come from 1987 muon data.

contents of the plots in figure 3 and then calculates equation (4) is available, and is thoroughly described in the Vax file

FNAL::USR$ROOT:[DSMITH.DIF]CMDIF.DOC .

4 Charge Asymmetry

The small absorption cross section for positive kaons leads to an excess of positive tracks in the central muon chambers. Charge symmetric contributions to the central muon rate, such as decay-in-flight or prompt muons, will decrease the observed asymmetry. An earlier CDF note [3] set limits on the magnitude of the asymmetry by making broad assumptions about the contribution from decay-in-flight. Now we are in a position to refine the prediction.

Figure 6 shows the ratio

$$R(p_t) = \frac{N_+(p_t)}{N_-(p_t)}$$

where $N_+(p_t)$ and $N_-(p_t)$ are the numbers of positive and negative tracks observed in the central muon chambers, as a function of transverse momentum. The solid curve uses the results of the monte carlo simulation to calculate the number of tracks coming from muon decay. The dashed curve does not include the dE/dx correction. Only non-interactive punchthrough, taken from reference [3], and decay-in-flight are considered. R is an overestimate of the observe The fraction of kaons and protons in the charged track spectrum in the CTC is taken to be $\frac{K}{\pi} = \frac{(p+\bar{p})}{\pi} = 0.10$.

Also shown in figure 6 are points from 1987 muon data, using the tight cuts of table 2. The agreement is close but not perfect. At the lowest p_t, a technical hurdle causes an overestimate

of the asymmetry. Correcting this point requires considerable additional work and did not seem worthwhile. At higher p_t, other effects may contribute:

- We have considered only non-interactive punchthrough and decay-in-flight. A minimum ionizing cut on the data removed most shower leakage (interactive punchthrough), but the remaining contribution will diminish the observed asymmetry;
- The $\frac{K}{\pi}$ mixture of the parent spectrum is poorly understood but is probably greater than 0.10. Increasing $\frac{K}{\pi}$ increases the predicted asymmetry;
- Cosmic rays and prompt muons make small contributions to the data sample we used, but both diminish the observed asymmetry and they are not included in the prediction. Track misassociation, where a muon stub is matched with the wrong central track, is another possible background.

In spite of these shortcomings, the data and the prediction agree qualitatively and we conclude that the asymmetry is a useful tool for understanding the single muon data.

5 Conclusions

A general method for calculating decay-in-flight rates in the central muon chambers shows that the contribution from π decay falls off more quickly (as a function of p_t) than the contribution from K decay, so that for reasonable input spectra and hadron mixes, the two rates become comparable in the p_t = 5-10 GeV/c range. By 15 GeV/c, decay-in-flight is a small background for central muon studies. Combining the decay-in-flight study with earlier non-interactive punchthrough results leads to a prediction of the charge asymmetry that compares favorably with 1987 muon data.

References

1. "The CDF Central Muon Detector", G. Ascoli et al, *Nucl Instr and Meth* **A268** (1988) 33.
2. "Kaon Production in $p\bar{p}$ Collisions at a Centre-of-Mass Energy of 540 GeV", G.J. Alner et al (UA5 collaboration) *Nucl Phys* **B258** (1985) 505.
3. "Pion Punchthrough Probability of the Central Calorimeter Wedges",D.A. Smith and H.B. Jensen, CDF note #707 (August 1988).
4. "Pion and Kaon Decay in the CTC Volume Faking a high p_t Track", John Skarha, CDF-587 (1987).